Experimental analysis on the influence of freeform bending on Barkhausen noise for steel tubes

Daniel Maier, Lorenzo Scandola, Matthias Werner, Sophie Stebner, Ahmed Ismail, Boris Lohmann, Sebastian Münstermann, Wolfram Volk, Philipp Lechner

Angaben zur Veröffentlichung / Publication details:

Maier, Daniel, Lorenzo Scandola, Matthias Werner, Sophie Stebner, Ahmed Ismail, Boris Lohmann, Sebastian Münstermann, Wolfram Volk, and Philipp Lechner. 2023. "Experimental analysis on the influence of freeform bending on Barkhausen noise for steel tubes." In *Material Forming: the 26th International ESAFORM Conference on Material Forming (ESAFORM 2023), April 19-21, 2023, Kraków, Poland*, edited by Lukasz Madej, Mateusz Sitko, and Konrad Perzynski, 2091–2100. Millersville, PA: Materials Research Forum LLC. https://doi.org/10.21741/9781644902479-224.

Materials Research Proceedings 28 (2023) 2091-2100 https://doi.org/10.21741/9781644902479-224

Experimental analysis on the influence of freeform bending on Barkhausen noise for steel tubes

MAIER Daniel[1, a*], SCANDOLA Lorenzo[1,b], WERNER Matthias[1,c], STEBNER Sophie[2,d], ISMAIL Ahmed[3,e], LOHMANN Boris[3,f], MÜNSTERMANN Sebastian[2,g], VOLK Wolfram[1,h] and LECHNER Philipp[1,i]

[1]Chair of Metal Forming and Casting, TUM School of Engineering and Design, Technical University of Munich, Germany

[2]Integrity of Materials and Structures, Department of Ferrous Metallurgy, RWTH Aachen University, Germany

[3]Chair of Automatic Control, TUM School of Engineering and Design, Technical University of Munich, Germany

[a]daniel.maier@tum.de, [b]lorenzo.scandola@utg.de, [c]matthias.werner@utg.de, [d]sophie.stebner@iehk.rwth-aachen.de, [e]a.ismail@tum.de, [f]lohmann@tum.de, [g]sebastian.muenstermann@iehk.rwth-aachen.de, [h]wolfram.volk@utg.de, [i]philipp.lechner@utg.de

Keywords: Freeform Bending, FEM, Barkhausen Noise, Softsensor, Closed-Loop Control

Abstract. Freeform bending with a movable die makes it possible to bend complex structures and seamless radii without changing the bending tools. Currently, most research focuses on minimizing the geometrical deviations without considering the mechanical properties of the bent tubes. A previous work showed, that the geometry can be decoupled from the mechanical properties with non-tangential bending [1]. The implementation of a soft sensor based on ultrasonic contact impedance measurements (UCI) of the property-controlled freeform bending has also been examined [2], as well as a structure for closed-loop control based on material properties [3]. The present work deals with a micro-magnetic sensor and Barkhausen noise (BHN) and investigates its suitability for the closed-loop control. For this purpose, different processing routes for freeform-bent steel tubes are experimentally investigated by their characteristic BHN. In addition to an existing simulation model, a data basis for the impact of freeform bending parameters is built to extend the existing model of a property-based closed-loop control.

Introduction

Freeform bending with a movable die is a forming technology that allows the bending of complex three-dimensional tube geometries without changing the bending die. The accuracy of the bending process depends on the tolerances and fluctuations in the mechanical properties as well as the tolerances of the process (e.g., friction, etc.). These disturbances significantly influence the bent part. In addition, inadequate knowledge of the mechanical properties before and after the bending process can lead to deviations in downstream processes. This leads to the conclusion, that there is a need for closed-loop control based on the mechanical properties of the tube, to reduce failures as well as scrap and to improve the quality of freeform-bent parts.

Non-tangential bending allows the decoupling of the geometry and mechanical properties [1]. In order to control the mechanical properties during the freeform bending process, a suitable measuring system must be available in addition to the intervention in the kinematics of the bending die. This paper provides an experimental analysis of the influence of freeform bending process parameters on BHN for steel tubes. Therefore, different states of the steel tubes (unbent, bent,

unbent and annealed, annealed and bent) are measured with a micro-magnetic sensor and the BHN is analyzed. Furthermore, tubes formed with the new concept of non-tangential bending are under investigation. Ultimately, the results are compared to the numerical model to check the congruence between the numerical model and measurements on real bent tubes.

State of the Art

Freeform bending with a movable die is a process that has been investigated to a large extend. Most of the research focuses on improving the geometrical accuracy of the freeform-bent part, but only a few investigate the mechanical properties during the bending process. [4] showed that the manufacturing strategy of roll-formed tubes influences the material properties and the subsequent bending process. There have also been investigations that analyze the influence of different process parameters on the bending result in freeform bending using numerical simulations [5]. Numerical simulations are often used to get a better understanding of the freeform bending process. [6] showed two models for freeform bending with three and five degrees of freedom and a simulation model for rotary draw bending. Both round tubes and profiles were bent using these models. Another simulation model for freeform bending as the preform forming step of hydroforming was also investigated [7]. A simulation model is used to calculate the motion profile of the bending die to get better geometrical accuracy results while reducing scrap [8]. If only a 2D bending part is manufactured, the hole part can be described by the parameters radius and bending angle. In freeform bending there is a process-related, complex transition between straight tube segments and the area of constant curve curvature due to the particular motion profile of the bending die [9]. Accordingly, the specified bending radius is determined by means of regression only in the region of constant curve curvature [10]. The bending angle is calculated from the direction vectors of approximated straight lines at the beginning and end of the bent part. Automatic extraction of the bending line from discrete data and vice versa makes this analysis much faster and more efficient [11]. In terms of influencing factors, [12] conclude with numerical simulations and validation experiments that the yield strength affects the forming limit and wrinkling instability. The results also showed that friction and clamping pressure have a smaller impact on the forming limit compared to the axial propulsion speed and the gap between the tubes and bending die. The concept of [13] shows that a kinematic bending process can be controlled. A concept for both direct and indirect control of torque superposed spatial bending was presented in their work.

Different approaches are pursued to optimize the bending processes using the extended Kalman filter (EKF) in particular. On the one hand, it is used to predict the trajectory during freeform bending and thus to optimize the process and the process parameters [14]; on the other hand, the EKF is also used in the field of stress prediction and closed-loop control during freeform bending [1]. There have also been investigations into BHN measurements to analyze the residual stresses. BHN is affected by residual stresses to the same extent as it is by the microstructure, but a careful calibration process is necessary to get a good correlation between stresses and BHN [15]. BHN has also been installed in a broaching machine tool to conduct in-situ measurements during the orthogonal cutting process, and a correlation between the residual stress and the detected BHN signal was evaluated [16]. Another study showed that the reciprocal of the peak amplitude of the BHN has a linear relationship with the stresses [17]. Therefore, tensile tests with carburized SAE 9310 and 32CDV13 were applied. For low-frequency BHN measurements near the surface, it was shown that in case-carburized steel, the residual stresses change differently compared to the subsurface in response to the prior applied tensile or compressive stresses [18]. Although BHN has been the subject of numerous studies, the results are difficult to compare because most studies differ in terms of the material and samples used [19]. Therefore, it can be concluded that a better understanding of how different factors influence BHN is still needed.

As the state of the art indicates, BHN is suitable for measuring different specimens and a range of materials. In addition, it is also shown that freeform bending with its many degrees of freedom

is a suitable controllable process. Overall, the great need for closed-loop control based on the mechanical properties of the tube during freeform bending can clearly be seen.

Materials and Methods

This paper deals with the experimental analysis of the influence of residual stresses in the raw material on the geometry and BHN of freeform-bent steel tubes. The aim is to show that different stress states can be measured using a micro-magnetic sensor and analyzed using BHN. In addition, it will be shown that different stress states influence the resulting bent part. Due to the kinematic forming process and the associated many degrees of freedom, freeform bending with a movable die is particularly suitable for influencing the mechanical properties.

Freeform bending machine and tubular raw material. In this article, all experiments are performed using a 6-axis freeform bending machine with a movable die, built by J. Neu GmbH (Grünstadt). The machine has six degrees of freedom, of which three are translational and three are rotational. Fig. 1 shows the six degrees of freedom and all relevant parts of the freeform bending machine.

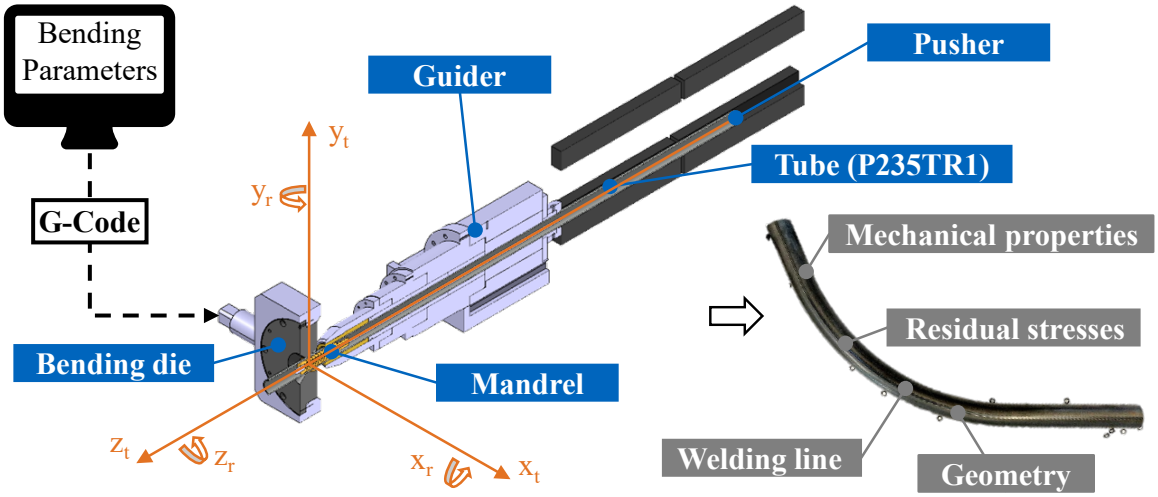

Fig. 1. Principal of freeform bending with movable die and the resulting bent part [1].

To produce a freeform-bent part, a round tube must first be inserted into the machine. The tube is then advanced along the z-axis at a constant speed. The tube is pushed over the bending mandrel and through the bending die. In addition to the feed, the die starts to move. The bending die can be deflected in the xy-plane and can rotate around all three axes (x-, y- and z-axis), performing the movements simultaneously. To bend a tube, as shown in Fig. **1**, the bending die is deflected and rotated to its maximum position, then stops and remains in the maximum deflected position until the bending angle is reached, and then returns to the starting position. This entire process occurs while the tube is being constantly advanced. The kinematic process can therefore be divided into three sections: the transition, the constant and return sections. For a more detailed understanding of the process, the authors refer to detailed studies of the freeform bending process [1-3, 7, 8].

For the experimental investigations in this paper, welded steel tubes made of P235 are used. The circular steel tubes have an outer diameter of 42.4 ± 0.5 mm, a thickness of 2.6 ± 0.3 mm and a length of 800 ± 2 mm with an evenly finished weld seam. The tubes are manufactured according to the international norms EN 10217-1 and EN 10219-1. The steel tubes have been used in other investigations and are already described in detail [1, 2, 20].

Analysis of bending geometry and Barkhausen noise signal. To analyze the geometry of the parts, a three-dimensional triangular surface mesh of the part is created by an optical measurement system with a handheld laser sensor. The bend angle is determined by fitting a cylinder at each

end of the tube and then measuring the angle between the two centerlines. To analyze the curvature, several sections are created along the longitudinal direction of the tube, and a circle is fitted through each section. The centers of all fitted circles are then connected, resulting in the centerline of the bent part. The curvature of the centerline is then calculated and evaluated. The curvature is divided into the same three sections as dictated by the kinematics of the bending tool (transition section, constant section and return section) and a non-bent section at the beginning and end of each tube.

To measure and analyze the BHN, a micro-magnetic sensor named *µmagnetic* in interaction with the software *Optimizer4D* from QASS GmbH (Wetter) is used. As BHN is a non-destructive testing method measurement method with high sampling rates, it is advantageous compared to other stress measurement methods, such as the hole drilling method. Since the BHN can be influenced by a gap between the sensor and workpiece, the sensor is placed directly on the tube to neglect this influence. To avoid short-circuiting or overdriving the BHN, a tape covers the sensor and, at the same time, minimizes the distance between the sensor and the tube. The sensor measures the inductive current, and the results are subsequently visualized using a Fourier transformation. The 3D landscape of the measurement signal consists of the axes frequency, time and amplitude. The process flow for the downstream signal processing of the BHN is shown in Fig. 2.

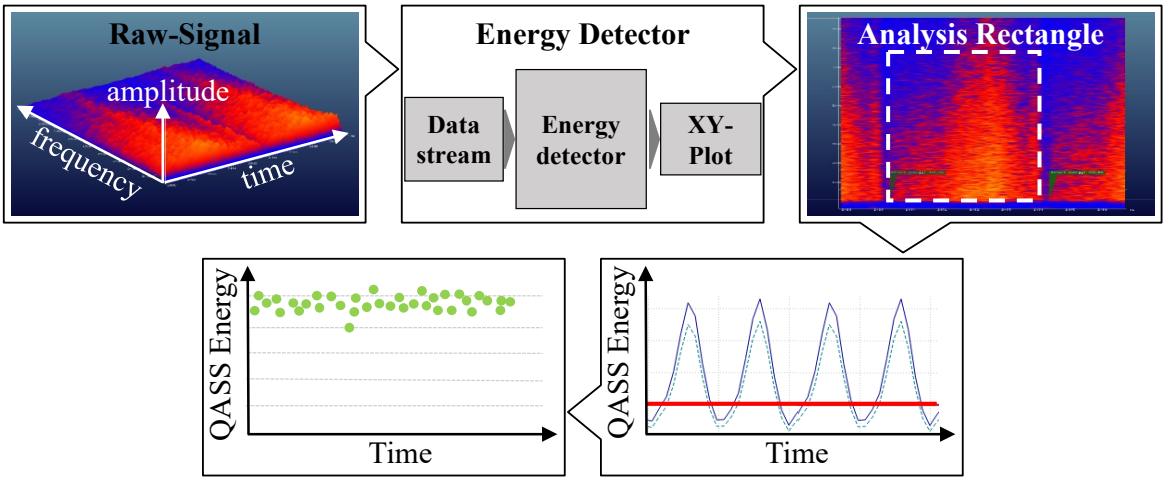

Fig. 2. Process flow for measuring and analyzing the MBH.

An analysis network with a so-called “energy detector” is used to analyze the Fourier-transformed BHN signal. It finds contiguous ranges of a certain minimum energy in a signal. The energy is calculated within a rectangular window (in time and frequency), which is successively shifted forward in time. Neighboring windows in which an energy threshold is exceeded are combined to form a pattern. This pattern is analyzed with respect to the mean value and standard deviation for each measurement point. To ensure a high penetration depth, an excitation frequency of 200 Hz and magnetizing voltage of 700 mV is set. At higher frequencies, the penetration depth is reduced. The *Optimizer4D* software offers an energy-related value in both the time and frequency axes, which is called QASS energy. This value cannot be expressed by the SI-unit system and is, therefore, given later on without a unit [16].

Strategy. The focus is on the influence of the stress state of the raw material in freeform bending and the suitability of the micro-magnetic sensor for inline measurement of property changes during freeform bending. Therefore, different conditions of the unbent tube are investigated, as well as freeform bending experiments with different starting conditions (see Fig. 3). With these experimental investigations and bending strategies, some research questions arise:

1. Can disturbances in the unbent raw material be measured with BHN and is there a difference compared to annealed raw material?
2. How does annealing influence freeform-bent tubes in terms of geometry and BHN?
3. Is it possible to measure a different BHN in non-tangential freeform-bent tubes?

This paper tries to find answers to these research questions by carrying out experimental investigations and micro-magnetic measurements on freeform-bent steel tubes.

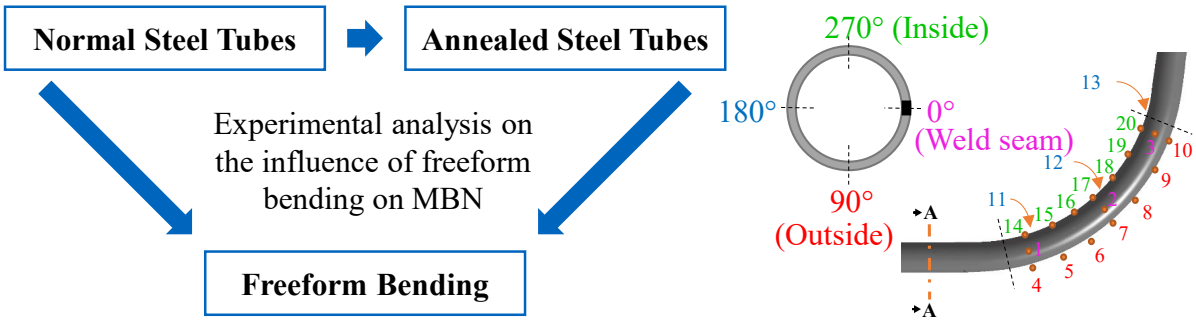

Fig. 3. Big picture and schematic depiction of measurement points on the unbent and bent part.

Experimental Investigations

This section describes the experimental investigations starting with residual stress annealing the unbent tubes, followed by the freeform bending process with a movable die, and the BHN measurement and analysis methods.

Residual stress annealing.

Residual stress annealing is used to minimize the residual stresses within the unbent tube. Table 1 shows the exact annealing parameters for the steel tubes made from P235. The annealing parameters were also part of other investigations with the same tubes [1].

Table 1. Residual stress annealing parameters for the experimental investigations.

Temperature	$T_0 \rightarrow$ 620 °C	620 °C	620 °C → T_0
Time	2 h	2 h	48 h

Fig. 4 shows the microstructure of the base material for normal and annealed tubes, based on the investigations of [1].

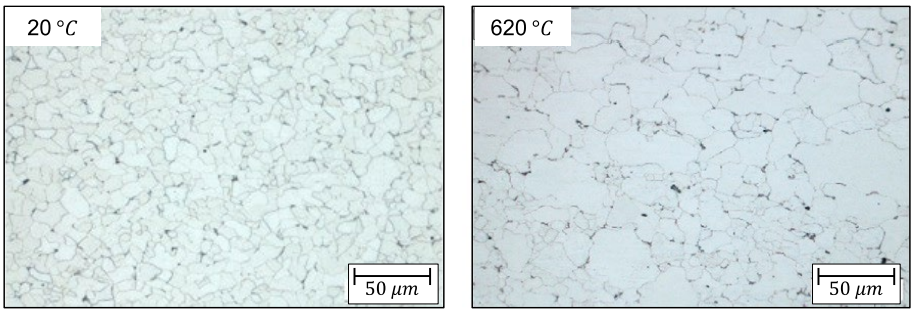

Fig. 4. Light microscopic image of the microstructure at x500 magnification Left: base material, Right: residual stress annealed [1].

Freeform bending and Barkhausen noise measurement. After the residual stress annealing, all tubes (normal and annealed) are bent with the freeform bending machine. Two different bending strategies are used. The first bending strategy includes five different part geometries (V01 - V05), where all result in a different curvature and bending angle. The second bending strategy includes seven different kinematics using the non-tangential bending technology [1]. This results in bent

parts with the same geometry but different residual stresses, according to [1]. The maximum deflection y_{max} and rotation φ_{max} of the bending die for all experiments are listed in Table 2.

Table 2. Freeform-bent parts with deflection and rotation of the bending die.

Name	**V01**	**V02**	**V03**	**V04**	**V05**		
y_{max}	5.85 mm	7.47 mm	9.85 mm	13.29 mm	18.15 mm		
φ_{max}	9.83 °	12.32 °	15.79 °	20.39 °	26.11 °		
Name	**A01**	**A02**	**A03**	**A04**	**A05**	**A06**	**A07**
y_{max}	9.00 mm	10.00 mm	10.00 mm	11.00 mm	11.00 mm	12.00 mm	12.00 mm
φ_{max}	22.00 °	16.00 °	20.00 °	13.00 °	14.00 °	12.00 °	13.00 °

The unbent (normal and annealed) and the bent tubes are measured at several measuring points with the micro-magnetic sensor; see Fig. 3. There are three measuring points on the sides of the tube, with one side corresponding to the weld seam (0°). On the inside (270°) and outside (90°), there are seven measuring points each since this is where the tube records the greatest possible deformation. Please note that all measurement points are on the constant section of the bent tube.

Results and Discussion

At the beginning, the unbent raw material and the annealed raw material are investigated by micro-magnetic measurements, and additionally, the influence of the annealing process on the geometrical dimensions of the unbent tubes is analyzed. Subsequently, the results of unbent tubes with and without prior annealing are described and discussed in terms of geometry and BHN. A distinction is made between tangentially and non-tangentially bent tubes for the bent components.

Unbent raw material.

There are two different conditions of the unbent material: normal and annealed. The annealing process has been carried out with the parameters shown in Table 1. Optical measurement technology was used to measure the surface of the tube and then evaluate the outer diameter (D_{Out}) and inner diameter (D_{In}). In addition, measurements were carried out with the micro-magnetic sensor at the positions shown in Fig. 3. The results are shown in Fig. 5.

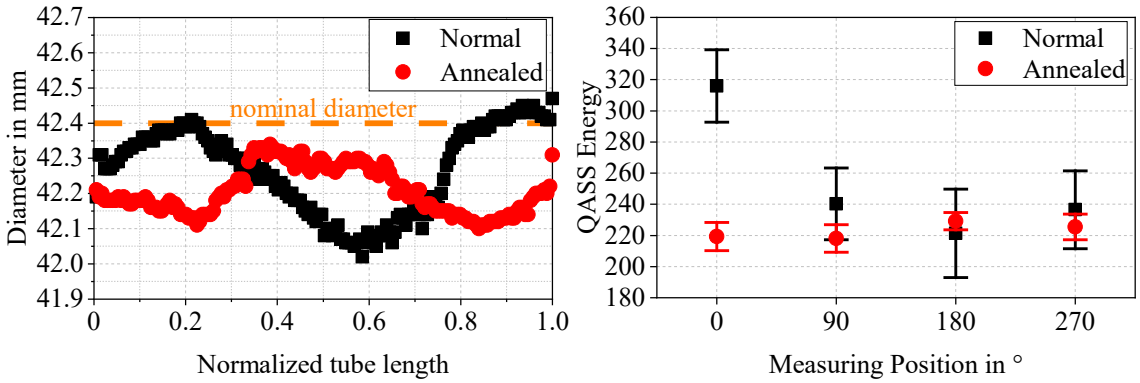

Fig. 5. Results for unbent tubes with and without residual stress annealing Left: Outer diameter, right: BHN.

For the outer diameter, it can be seen that all measurement points are within the desired tolerances (42.4±0.5 mm) for the normal and annealed tubes. The left side of Fig. 5 shows an example of a measured tube where the measuring points are distributed over the length. In addition, it appears that a trend reversal is occurring because of the annealing. At both ends, the normal tube

has a larger diameter than in the middle area, while the annealed tube shows the opposite trend. The deviation of the outer diameter is smaller after annealing compared to the normal material. The thickness of the material is within the tolerances (2.6±0.5 mm) for all measurement points. For geometrical tolerances, annealing has a positive impact due to the fact that the deviations become smaller.

On the right side of Fig. 5, the weld seam (0°) has a higher QASS energy level compared to the other measurement points for the normal tube. After annealing, the energy level of the weld seam decreases to approximately the same level as the other points. Because of the annealing process, the stresses throughout the tube were relieved, and the microstructure was affected. Fig. 4 shows significantly fewer grain boundaries in the annealed material, resulting in a lower QASS energy level. Overall, it can be stated that stress-relief annealing mainly affects the weld seam and results in a more homogeneous measurement signal with lower standard deviations.

Influence of bending process on BHN. Both unbent tube conditions (normal and annealed) are bent with the freeform bending machine and the exact same process parameters. The results are divided into the results for tangential bending (V01 - V05) and non-tangential bending (A01 - A07). The results are analyzed in comparison with numerical simulations based on a simulation model already described in [20].

In terms of geometry, it can be seen that the tubes made from the annealed material achieve higher constant curvature (equals smaller radii) than the non-annealed tubes, according to Fig. 6. This trend can be seen for all bent components V01 - V5 and A01 - A07. It can also be seen that for the non-tangential bent parts, approximately the same curvature results. This validates that constant curvature is possible for various non-tangential bending setups and builds the foundation for the following investigations. Since no differences were found in the geometric dimensions of the unbent annealed tube compared to the normal unbent tube, the differences in the curvature must be attributed either to the reduced stresses or the changed microstructure and the associated material properties after the annealing process.

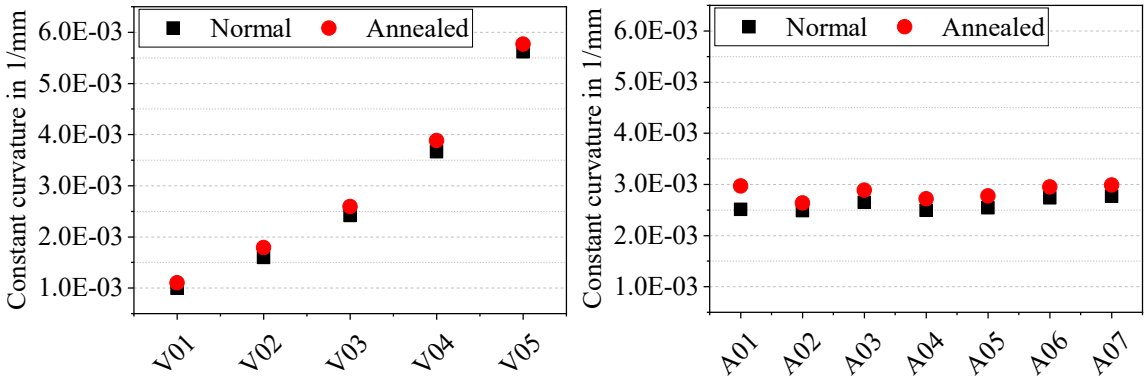

Fig. 6. Curvature of the freeform-bent parts made from normal and annealed straight tubes.

The results of the BHN analysis for the outside of the freeform-bent parts V01 - V05 and the non-tangential bent parts A01 - A07 with and without annealed raw material are shown in Fig. 7. The figure also shows the von Mises stresses determined by numerical simulations using the same measurement points as in the real bending investigations. In all tests and in the simulation, the results on the inside scatter strongly, which is why the evaluation concentrates only on the outside.

Fig. 7 shows that the BHN measurements for annealed tubes have greater fluctuations than the BHN results of normal tubes. A similar trend can be seen in the results of the annealed tubes and the simulation. With increasing curvature, the QASS energy level in the annealed tubes and the von Mises stresses determined in the simulation increase. This behavior is also to be expected due

to the bending process because the greatest strain occurs at the greatest curvature, which increases the stresses. The increase in the BHN can be explained by the fact that predominantly tensile stresses are expected on the outside of the bent tube, and these stresses increase the intensity of the BHN. Compressive stresses, on the other hand, reduce the intensity of the BHN. Only test V03 does not fit well with this trend. In contrast, this trend cannot be seen in the normal tubes. Here it seems like the QASS energy level decreases with increasing curvature. This allows the assumption that the stresses induced in the base material run counter to the stresses introduced by the freeform bending process. The fact that the results of the simulation fit better to the annealed tubes than to the normal tubes is because in the simulation, bending is done with a tube where the initial stress state is zero. The annealing reduces the stresses, and therefore the simulation corresponds more to these experiments.

In the following section, the results of non-tangential bending are examined in more detail. The quintessence of non-tangential bending is the introduction of different stress states at constant geometry. If we look at Fig. 7 together with Fig. 6, we can see exactly this relationship. Significant differences can be seen in both the simulations and the measured freeform-bent parts. On the outside, for example, the highest QASS energy level (A03) is more than 10% higher than the lowest (A01). In contrast to the previous results, a similar trend for the non-tangentially bent components can be seen between normally bent tubes and the simulation. The annealed tubes also fit with this trend, except for the outlier at A03. In the context of the BHN, the results show that as stresses decrease, the BHN also decreases, and as stresses increase, the BHN increases. Based on the results shown, it can be said that the sensor used and the BHN are suitable for measuring different stresses during freeform bending. However, in order to be able to use the sensor in a property-based control loop, a correlation of the BHN with the real stresses in the bent part must still be created. In addition, the magnetization parameters must be further refined in order to determine the various influences on freeform bending as much as possible, even in an inline measurement.

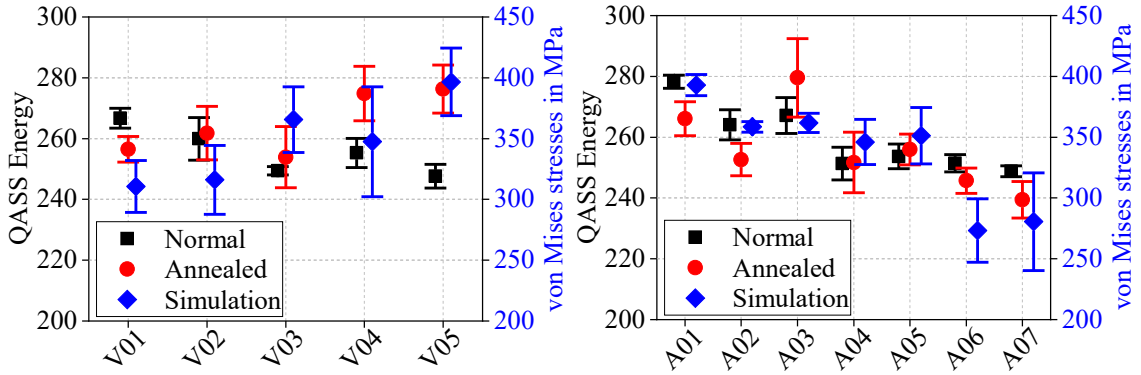

Fig. 7. Resulting BHN on the outside of freeform-bent tubes in comparison to von Mises stresses determined in numerical simulations. Left: tangential bending, right: non-tangential bending.

Summary

In the present work, the influence of different initial conditions in the tubes during freeform bending on the geometry and BHN was investigated. For this purpose, a series of tests were carried out with annealed and non-annealed tubes, which were then measured and evaluated with the micro-magnetic sensor. In addition, the results were compared with the results from the simulation. The following findings can be noted in relation to the research questions defined at the beginning of the study:

- Different QASS energy levels were found in the circumferential direction of the tube, with the weld seam significantly above the base material. The energy levels of the base material were all within a certain scatter band, which is reduced by annealing.

- In terms of geometry, it was found that the annealed tubes lead to smaller radii compared to non-annealed raw material. In terms of BHN, the annealed tubes showed better accordance with the simulation result and the presented theory.
- In non-tangential bending, it is possible to decouple the mechanical properties from the geometry. The differences in the non-tangentially bent tubes could be measured with BHN, showing a similar trend in the normal and annealed results as in the simulations.
- The micro-magnetic sensor can measure differences in freeform-bent parts, and the results are in good accordance with the simulation model. With these results, it can be said that the sensor can be used to measure BHN quickly and use the results in order to control the freeform bending process based on its properties.

For future work the parameters of the micro-magnetic sensor need to be optimized for the given steel tubes in order to measure more accurately. In addition, a correlation between the BHN and residual stresses is necessary to get a better understanding of the process and to control the bending process.

Acknowledgement
This work was supported by the German research foundation (DFG) under grant number [424334318].

References
[1] D. Maier, S. Stebner, A. Ismail, M. Dölz, B. Lohmann, S. Münstermann, W. Volk, The influence of freeform bending process parameters on residual stresses for steel tubes, Adv. Industr. Manuf. Eng. 2 (2021) 100047. https://doi.org/10.1016/j.aime.2021.100047
[2] S.C. Stebner, D. Maier, A. Ismail, S. Balyan, M. Dölz, B. Lohmann, W. Volk, S. Münstermann, A System Identification and Implementation of a Soft Sensor for Freeform Bending, Mater. 14 (2021) 4549. https://doi.org/10.3390/ma14164549
[3] A. Ismail, D. Maier, S. Stebner, W. Volk, S. Münstermann, B. Lohmann, A Structure for the Control of Geometry and Properties of a Freeform Bending Process, IFAC-PapersOnLine 54 (2021) 115-120. https://doi.org/10.1016/j.ifacol.2021.10.060
[4] N. Beulich, R. Mertens, J. Spoerer, W. Volk, Influence of tube rollforming on material properties and subsequent bending processes, Forming Technology Forum, 2019.
[5] N. Beulich, J. Spoerer, W. Volk, Sensitivity analysis of process and tube parameters in free-bending processes, IOP Conf. Ser.: Mater. Sci. Eng. 651 (2019) 12031. https://doi.org/10.1088/1757-899X/651/1/012031
[6] P. Gantner, D.K. Harrison, A.K. de Silva, H. Bauer, The Development of a Simulation Model and the Determination of the Die Control Data for the Free-Bending Technique, Proceedings of the Institution of Mechanical Engineers, Part B: J. Eng. Manuf. 221 (2007) 163-171. https://doi.org/10.1243/09544054JEM642
[7] N. Beulich, P. Craighero, W. Volk, FEA Simulation of Free-Bending - a Preforming Step in the Hydroforming Process Chain, J. Phys.: Conf. Ser. 896 (2017) 12063. https://doi.org/10.1088/1742-6596/896/1/012063
[8] M.K. Werner, D. Maier, L. Scandola, W. Volk, Motion profile calculation for freeform bending with moveable die based on tool parameters, ESAFORM 2021, 2021. https://doi.org/10.25518/esaform21.1879
[9] S. Groth, B. Engel, K. Langhammer, Algorithm for the quantitative description of freeform bend tubes produced by the three-roll-push-bending process, Prod. Eng. Res. Devel. 12 (2018) 517-524. https://doi.org/10.1007/s11740-018-0795-2
[10] N. Chernov, Circular and Linear Regression: Fitting circles and lines by least squares. [S.l.]: CRC PRESS, 2020.

[11] L. Scandola, D. Maier, M. Konrad Werner, C. Hartmann, W. Volk, Automatic Extraction and Conversion of the Bending Line from Parametric and Discrete Data for the Free-Form Bending Process, in The Minerals, Metals & Materials Series, NUMISHEET 2022, K. Inal, J. Levesque, M. Worswick, C. Butcher (Eds.), Cham: Springer International Publishing, 2022, pp. 813-826.
[12] W. Wei, H. Wang, H. Xiong, X. Cheng, J. Tao, X. Guo, Research on influencing factors and laws of free-bending forming limit of tube, Int. J. Adv. Manuf. Technol. 106 (2020) 1421-1430. https://doi.org/10.1007/s00170-019-04692-0
[13] D. Staupendahl, S. Chatti, A.E. Tekkaya, Closed-loop control concept for kinematic 3D-profile bending, in Nantes, France, 2016, p. 150002.
[14] J. Wu, B. Liang, J. Yang, Trajectory prediction of three-dimensional forming tube based on Kalman filter, Int. J. Adv. Manuf. Technol. 121 (2022) 5235-5254. https://doi.org/10.1007/s00170-022-09521-5
[15] S. Schuster, L. Dertinger, D. Dapprich, J. Gibmeier, Application of magnetic Barkhausen noise for residual stress analysis - Consideration of the microstructure, Mater. Test. 60 (2018) 545-552. https://doi.org/10.3139/120.111186
[16] K. Shimosaka, T. Bergs, D. Schraknepper, S. Münstermann, M. Meurer, In-situ Evaluation of Surface Integrity Modifications by means of Barkhausen Noise Measurement, Procedia CIRP 102 (2021) 465-470. https://doi.org/10.1016/j.procir.2021.09.079
[17] L. Mierczak, D.C. Jiles, G. Fantoni, A New Method for Evaluation of Mechanical Stress Using the Reciprocal Amplitude of Magnetic Barkhausen Noise, IEEE Trans. Magn. 47 (2011) 459-465. https://doi.org/10.1109/TMAG.2010.2091418
[18] V. Moorthy, B.A. Shaw, S. Day, Evaluation of applied and residual stresses in case-carburised En36 steel subjected to bending using the magnetic Barkhausen emission technique, Acta Mater. 52 (2004) 1927-1936. https://doi.org/10.1016/j.actamat.2003.12.034
[19] S. Santa-aho, A. Laitinen, A. Sorsa, M. Vippola, Barkhausen Noise Probes and Modelling: A Review, J. Nondestruct. Eval. 38 (2019). https://doi.org/10.1007/s10921-019-0636-z
[20] S.C. Stebner, D. Maier, A. Ismail, M. Dölz, B. Lohman, W. Volk, S. Münstermann, Extension of a Simulation Model of the Freeform Bending Process as Part of a Soft Sensor for a Property Control, Key Eng. Mater. 926 (2022) 2137-2145. https://doi.org/10.4028/p-d17700